J Gastroenterol (2012) 47:805–813
DOI 10.1007/s00535-012-0546-7

ORIGINAL ARTICLE—LIVER, PANCREAS, AND BILIARY TRACT

Carnosic acid (CA) prevents lipid accumulation in hepatocytes through the EGFR/MAPK pathway

Ting Wang · Yasuhiro Takikawa · Takahito Tabuchi · Takumi Satoh · Kunio Kosaka · Kazuyuki Suzuki

Received: 25 August 2011 / Accepted: 4 January 2012 / Published online: 18 February 2012

Abstract
Background Carnosic acid (CA), found in rosemary, has been reported to have antioxidant and anti-adipogenic properties. We recently demonstrated that CA protects against steatosis in *ob*/*ob* mice. In the present report, we investigated the molecular mechanism by which CA inhibits lipids accumulation both in vivo and in vitro.
Methods In the in vivo study, *ob*/*ob* mice were fed a standard chow diet with or without CA for 5 weeks, then their hepatocyte lipid accumulation was determined. The serum concentrations of cytokines, the levels of lipid regulatory mediators, and the hepatic metabolic and signaling molecules were also evaluated. In the in vitro study, HepG2 cells were used to further clarify the effects of CA on cellular lipid accumulation and to confirm the signaling pathways involved in these effects.
Results CA significantly reduced hepatocyte lipid accumulation. This effect was associated with repressed levels of hepatic PPARγ, reduced expression of inflammatory cytokines such as IL-1β, IL-12, IL-17, IFN-γ, MCP-1, and MIP-1β, and increased ATP, acetyl CoA, NAD(P)$^+$, and NAD(P)H. Other signaling molecules, such as EGFR, MAPK, AMPK, and ACC, which regulate lipid metabolism, were activated in mice fed the CA diet. CA inhibited palmitate-induced cellular lipid accumulation and stimulated the phosphorylation of both EGFR and MAPK. Pretreatment with either the EGFR inhibitor AG1478 or the MEK-specific inhibitor U0126 abolished the effects of CA on cellular lipid accumulation and decreased both the protein expression and activity of PPARγ.
Conclusions EGFR/MAPK signaling plays an important role in the inhibitory effect of CA on hepatocyte lipid accumulation.

Keywords Carnosic acid · Cellular lipid accumulation · PPAR · EGFR/MAPK signaling

Abbreviations

ACC	Acetyl CoA carboxylase
AMPK	AMP-activated protein kinase
ATP	Adenosine triphosphate
CA	Carnosic acid
EGFR	Epithelium growth factor receptor
FAS	Fatty acid synthase
FFA	Free fatty acid
G-CSF	Granulocyte colony-stimulating factor
GMCSF	Granulocyte macrophage colony-stimulating factor
GSH	Glutathione
IFN	Interferon
IL	Interleukin
MAPK	Mitogen-activated protein kinase
MCP-1	Monocyte chemotactic protein
MIP	Macrophage inflammatory protein
NAFLD	Nonalcoholic fatty liver disease
NF-κB	Nuclear factor-kappa B
PPAR	Peroxisome proliferation activator receptor
SREBP-1	Sterol regulatory element-binding protein-1

T. Wang · Y. Takikawa (✉) · K. Suzuki
Department of Gastroenterology and Hepatology,
Iwate Medical University, Morioka, Iwate, Japan
e-mail: ytakikaw@iwate-med.ac.jp

T. Tabuchi · T. Satoh
Department of Welfare Engineering, Faculty of Engineering,
Iwate University, Morioka, Iwate, Japan

K. Kosaka
Research and Development Center, Nagase Co., Ltd.,
Kobe, Japan

TG	Triglyceride
TGFβ1	Transforming growth factorβ1
TZDs	Thiazolidinediones
UCP2	Uncoupling protein 2
WAT	White adipose tissue

Introduction

Hepatic steatosis is an initial and critical step in the development of fatty liver diseases such as nonalcoholic fatty liver disease (NAFLD). Hepatocytes with an excessive triglyceride (TG) content may also present inflammation, insulin resistance, fibrosis, and even carcinogenesis [1]. Preventing the hepatocytes from accumulating fat is therefore the most effective way to block the progression of NAFLD to nonalcoholic steatohepatitis (NASH).

Although there are a variety of conditions that increase the amount of hepatic lipids, de novo lipogenesis and fatty acid β-oxidation are important for maintaining the balance of hepatic lipid metabolism [2–4]. Molecules such as AMP-activated protein kinase (AMPK) and peroxisome proliferation activator receptor (PPAR) γ, which participate in regulating these two processes, have thus attracted a lot of interest. AMPK, a serine threonine kinase with a catalytic α subunit and regulatory β and γ subunits, has been identified to be a major regulator of glucose and lipid metabolism and represents an attractive target for therapeutic intervention in the treatment of hepatic disorders [5]. AMPK activation depends on the phosphorylation of a subunit on threonine-172 (Thr-172) by kinase LKB1 or CaMKKβ. The activation of hepatic AMPK leads to increased fatty acid oxidation and simultaneously inhibits hepatic lipogenesis, cholesterol synthesis, and glucose production [6]. The actions of AMPK are attributed to its direct phosphorylation and the inactivation of a number of metabolic enzymes, including acetyl CoA carboxylase (ACC), which is a key enzyme regulating both fatty acid synthesis and β-oxidation. In addition, AMPK activation reduces the expression of sterol regulatory element-binding protein-1 (SREBP-1) c, which is the predominant SREBP-1 isoform in the liver, and which transcriptionally regulates lipogenesis [5–7].

PPARγ is another target for the treatment of NASH because it plays a role in increasing insulin sensitivity [8]. PPARγ agonists, such as thiazolidinediones (TZDs), have been proposed to improve insulin sensitivity by increasing the expression and release of adiponectin, an adipokine that activates AMPK. However, as a lipogenic gene, PPARγ enhances fat accumulation in adipose tissue by stimulating adipocyte differentiation, and in the liver, hepatic PPARγ regulates triglyceride homeostasis and contributes to hepatic steatosis [8, 9]. PPARγ is phosphorylated and inactivated by the extracellular receptor kinase–mitogen-activated protein kinase (ERK–MAPK) pathway. The MAPK phosphorylation site was mapped to serine-82 of mouse PPARγ1, which corresponds to serine-112 of mouse PPARγ2. The treatment of macrophages with transforming growth factor (TGF) β1 increases PPARγ phosphorylation and decreases TZD-induced CD36 expression via activation of the ERK–MAPK pathway [10]. In addition, MAPK has been demonstrated to inhibit the differentiation of 3T3–L1 fibroblasts to adipocytes through repression of the transactivation function of PPARγ [11]. However, whether MAPK plays a role in regulating PPARγ in hepatocytes remains unclear.

We recently reported that carnosic acid (CA), an extract of rosemary leaves, prevented obesity, ameliorated steatosis of the liver, and improved the glucose tolerance in an NAFLD animal model [12]. In addition, rosemary extract is generally recognized as safe (GRAS) by the US Food and Drug Administration, and CA has been commercially used as the principal component of rosemary extract in various foods and supplements. These factors indicate that CA is a novel and potentially effective drug for the treatment of NAFLD and that it appears to be safe for human use.

Furthermore, the antioxidant effects of CA have been considered to be responsible for its biological activity [13]. It has been reported that CA protects neurons from free radicals and thereby shields the brain from ischemia. In addition, CA was found to stimulate Keap1/Nrf2 signaling, thus resulting in the production of antioxidants such as glutathione (GSH), thereby reducing oxidative stress [14, 15]. In addition, CA at 0.1–10 μM significantly inhibited preadipocyte 3T3L1 cells from differentiating into mature adipocytes through the same pathway [16].

In order to clarify the mechanism underlying the effects of CA on the lipid accumulation in hepatocytes, we first investigated the effects of CA on regulating inflammatory factors, lipid regulating mediators, and hepatic metabolic and signaling molecules in *ob*/*ob* mice. We then tested the possible signaling pathways involved in the activity of CA in vitro by using a cellular lipid accumulation model.

Materials and methods

Cell culture and treatment

Human hepatocellular liver carcinoma cells (HepG2) were grown in DMEM medium with 10% fetal bovine serum (FCS, Invitrogen). For cell treatment, a stock solution of CA (Nagase Co., Osaka, Japan) was prepared

in DMSO. A stock solution of sodium palmitate (Sigma-Aldrich Co., Japan) was dissolved in a bovine serum albumin/Hank's balanced salt solution (BSA/HBSS) mixture [17]. The in vitro model of cellular fat accumulation was established by treating HepG2 cells with palmitate as described previously [18]. Specific inhibitors of EGFR (AG1478), MEK (U0126), and AMPK (compound C) were purchased from Santa Cruz Biotechnology (Santa Cruz, CA, USA), Promega Corporation (Madison, WI, USA), and EMD Biosciences, Inc. (Darmstadt, Germany), respectively.

Animals and treatment

Four-week-old male obese leptin-deficient (*ob*/*ob*) mice were purchased from Charles River Laboratories Japan, Inc. (Yokohama, Japan). The mice were housed under a 12-h light–dark cycle in a temperature- and humidity-controlled environment. For the experiments, mice were randomly divided into two groups and were fed a standard chow diet with (CA+) or without (CA−) CA [0.05% (wt/wt), Nagase Co., Osaka, Japan] for 5 weeks. The mice were killed and tissues were sampled at the end of the experiment. Blood was collected by cardiac puncture, and serum samples were stored frozen at −20°C until the analysis by a Bioplex cytokine assay. Liver tissue was weighed and fixed in glutaraldehyde for an electron microscopy analysis. Frozen sections were used for the metabolome analysis (HMT com., Tsuruoka, Japan) and for the analyses of protein levels or activity. The use of mice in this study complied with the relevant guidelines based on the laws of Japan, and the study protocol was approved by the animal research committee of Iwate Medical University.

Electron microscopy

The livers were freshly isolated, perfused, and fixed with 2.5% glutaraldehyde. Tissue fragments were postfixed in 1% osmium tetroxide, dehydrated, and embedded in epoxy resin. Sections were cut for light microscopy (toluidine blue staining) and electron microscopy, which was performed on an electron microscope (H7100s, Hitachi, Tokyo, Japan). The total area of the lipid droplets in a randomly selected microscopic field was quantified by using the Image J software program (NIH, Washington D.C., USA). The average value for each group was then calculated.

Bioplex cytokine assay

The serum from mice was collected and analyzed by Bioplex cytokine assays (Bio-Plex Mouse Cytokine 18-Plex Panel, Bio-Rad Laboratories, Hercules, CA, USA), according to the manufacturer's protocol. We analyzed the serum for the concentration of interleukin (IL)-1, IL-2, IL-3, IL-5, IL-6, IL-9, IL10, IL-12, IL-13, IL-17, tumor necrosis factor (TNF) α, granulocyte colony-stimulating factor (G-CSF), granulocyte macrophage colony-stimulating factor (GMCSF), interferon (IFN) γ, macrophage inflammatory protein (MIP)-1β, and monocyte chemoattractant protein 1 (MCP-1).

Western blot analysis

Total protein was isolated from liver tissue or HepG2 cells by a total protein extraction kit purchased from BioChain Institute, Inc. (Hayward, CA, USA). The nuclear fraction was isolated using the Nuclear/Cytosol Fraction Kit from Biovision Research Products (San Francisco, CA, USA). A total of 20 μg protein from each sample was separated by 10% SDS-PAGE and electrotransferred onto a polyvinylidene difluoride membrane. Immunoblotting was performed by using specific antibodies against PPARγ, SREBP-1, Nrf2, UCP2, β-actin (Santa Cruz Biotechnology, Santa Cruz, CA), FAS (Sigma Aldrich Japan Inc, Tokyo, Japan), phospho-AMPKα, phospho-ACC, phospho-EGFR, and phospho-MAPK (ERK1/2, Cell Signaling Technology, Charlottesville, VA, USA). The immunoreactive bands were visualized with an enhanced chemiluminescence reagent (Amersham Biosciences, Buckinghamshire, UK).

Oil Red O staining

HepG2 cells were washed once in PBS and fixed with freshly prepared 4% formaldehyde in PBS for 15 min. Cells were stained with Oil Red O as described elsewhere [19]. Spectrophotometric quantification of the staining was performed by dissolving the stained oil droplets in the cell monolayers with 4% Nonidet P-40 in isopropanol for 5 min. Then the absorbance was measured at 520 nm.

PPARγ transcription factor assay

After the treatment, the nuclear fraction of HepG2 cells was prepared, and the specific transcription factor DNA binding activity of PPARγ was detected by an enzyme-linked immunosorbent assay (ELISA; Cayman Chemical Company, Ann Arbot, MI, USA) according to the manufacturer's instructions.

Statistical analysis

The statistical analysis was carried out using Student's *t* test for unpaired comparisons. A p value less than 0.05

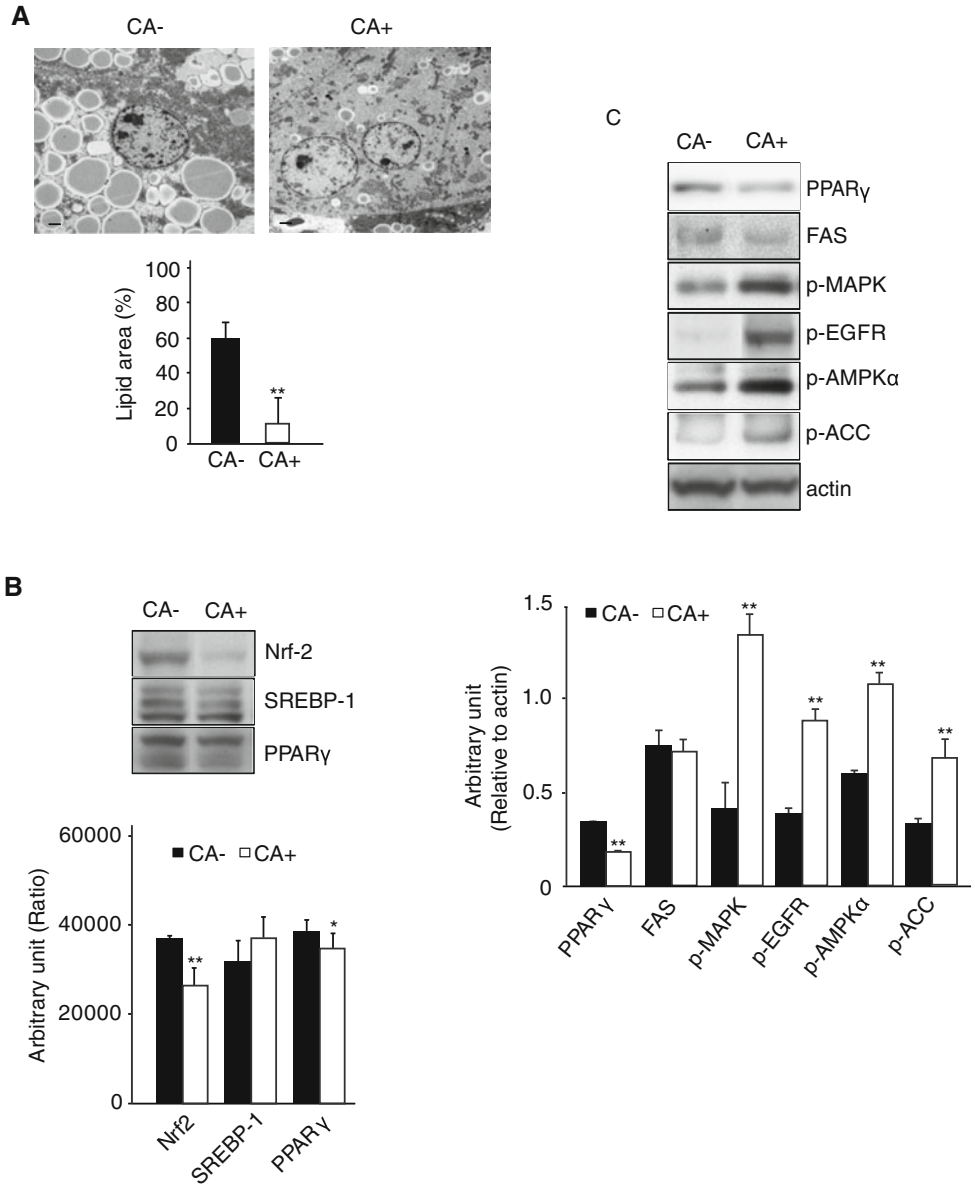

Fig. 1 Effects of CA treatment on hepatocyte lipid accumulation in *ob*/*ob* mice. **a** CA treatment inhibited hepatocyte lipid accumulation. Electron microscopy was performed and the results were quantified as described in the "Materials and methods". *Scale bar* 2 μm. **b** CA treatment significantly decreased the PPARγ protein level in the nuclear fraction of the liver. The nuclear fraction was extracted, and 20 μg of protein per sample was used for the Western blot analysis. **c** The effects of CA treatment on the protein levels of the signaling molecules involved in lipid metabolism. Tissue lysates (20 μg of total protein per sample) of liver samples were used for the Western blot analysis. The β-actin level was evaluated as a protein loading control. Representative results are shown. The quantitative data are presented as the means ± SD ($n = 3$ for **a** and $n = 5$ for **b**, **c**). $^{*}p < 0.05$, $^{**}p < 0.01$ versus the CA group

was considered to be significant. The results are presented as the means ± SD.

Results

CA reduces hepatocyte lipid accumulation in *ob*/*ob* mice

We previously reported that CA effectively reduced the total hepatic lipid content in *ob*/*ob* mice. In this study, we first detected the lipid accumulation in hepatocytes by electronic microscopy. As shown in Fig. 1a, the hepatocytes from control mice showed profound lipid accumulation. In comparison, CA feeding significantly decreased the fat accumulation in hepatocytes. In addition, lipogenic genes such as SREBP-1, fatty acid synthase (FAS), and PPARγ in liver nuclear fractions and/or in total lysates were subsequently examined. We observed that the PPARγ levels were significantly reduced in the mice fed the CA diet in comparison to the controls. In contrast, neither the amount of cleaved SREBP-1 (60–70 kDa) nor the FAS levels were significantly different between the two groups (Fig. 1b, c).

We then focused on the liver metabolites that correlated with the process of fatty acid β-oxidation. Compared with control mice, mice fed the CA diet showed increased levels of liver metabolites, such as NADH (3.1 times that of the control), NAD^{+} (3.3 times the control), acetyl CoA (1.7 times the control), ATP (2.6 times the control), and ADP (1.7 times the control), which are the major molecules that participate in the process of fatty acid β-oxidation (Table 1).

Table 1 Expression levels of hepatic metabolites involved in fatty acid β-oxidation and the NADPH-GSH system in *ob*/*ob* mice fed with or without CA

Metabolite	Relative area(/g)				Ratio
	CA−		CA+		CA+/CA−
FAD (divalent)	5.0 ± 0.27	10^{-1}	4.8 ± 0.52	10^{-1}	1.0
NADH	1.8 ± 0.70	10^{-1}	5.6 ± 0.29	10^{-1}	3.1
NAD^+	1.0 ± 0.8		3.3 ± 1.6		3.3
Acetyl CoA (divalent)	8.2 ± 0.48	10^{-2}	1.4 ± 0.31	10^{-1}	1.7
ATP	5.0 ± 0.38	10^{-1}	1.3 ± 0.21	10^{-2}	2.6
ADP	3.5 ± 1.6		5.8 ± 0.75		1.7
NADPH	2.1 ± 0.22	10^{-1}	4.1 ± 0.50	10^{-1}	2.0*
$NADP^+$	3.5 ± 0.96	10^{-1}	6.3 ± 1.4	10^{-1}	1.8
GSH	200 ± 9.8		200 ± 24		1.0
GSSG	34 ± 4.3		33 ± 4.4		1.0

*$p < 0.05$

Table 2 Serum concentrations of cytokines in *ob*/*ob* mice fed with or without CA

Cytokine	CA− (pg/mL)	CA+ (pg/mL)	Decrease (%)
IL-1α	1.3 ± 0.5	1.0 ± 0.3	23.1
IL-1β	176.0 ± 36.5	129.8 ± 32.4	26.3
IL-2	16.0 ± 3.4	13.7 ± 3.4	15.1
IL-3	41.7 ± 8.5	31.4 ± 6.2	24.7
IL-5	14.9 ± 4.2	10.6 ± 3.3	28.8
IL-6	4.1 ± 2.3	4.4 ± 6.0	−7.3
IL-9	373.1 ± 22.1	334.1 ± 33.4	10.5
IL-10	45.5 ± 8.6	40.1 ± 12.0	11.9
IL-12	152.0 ± 35.4	123.6 ± 35.7	18.7
IL-13	1160.8 ± 125.8	1047.6 ± 123.8	9.8
IL-17	55.3 ± 18.5	37.1 ± 7.5	32.9
IFN-γ	214.1 ± 25.9	161.7 ± 43.9	24.5
MCP-1	373.6 ± 39.7	309.7 ± 23.7	17.1
MIP-1β	46.4 ± 7.5	37.4 ± 11.9	19.4
TNF-α	271.9 ± 37.5	250.2 ± 50.5	8.0
G-CSF	60.3 ± 33.2	58.2 ± 43.8	3.5
GM-CSF	66.7 ± 10.6	53.1 ± 9.6	20.4

*$p < 0.05$, **$p < 0.01$

Activity of CA occurs independently of Nrf2/GSH signaling

In order to identify whether the Nrf2/GSH signaling pathway participates in the activity of CA, we evaluated the NADPH-glutathione (GSH) system in the livers of mice and detected the Nrf2 protein levels in the liver nuclear extracts. However, there were no significant differences in the levels of GSH in the present study, other than a significantly increased level of hepatic NADPH ($n = 3$, $p < 0.05$) in the mice fed the CA diet compared with controls (Table 2). Similarly, the CA treatment did not cause the expected increase in the Nrf2 levels in the liver nuclear fractions. On the contrary, the Nrf2 levels were decreased in the livers of mice fed the CA diet (Fig. 1b). Among the various molecules involved in lipid metabolism that were analyzed, both AMPKα and its downstream target, ACC, were activated in the livers of mice fed the CA diet in comparison to the controls. In addition, increased phosphorylation of both MAPK (ERK1/2) and its common upstream regulator, epithelial growth factor receptor (EGFR), was detected in the livers derived from the mice fed CA (Fig. 1c).

Reduction of lipid accumulation in HepG2 cells by CA is associated with EGFR and MAPK signaling

On the basis of the finding that CA feeding activated the phosphorylation of AMPK, EGFR, and MAPK, we examined the roles of these molecules in an in vitro model of cellular fat accumulation. As shown in Fig. 2a, HepG2 cells exhibited an excessive triglyceride accumulation after being induced by palmitate. The CA treatment significantly inhibited the effect of palmitate, however, co-treatment with a specific selective inhibitor of the EGFR (AG1478) or an inhibitor of the upstream effector of MAPK, MEK (U0126), recovered their cellular lipid accumulation (Fig. 2b). Furthermore, CA treatment stimulated the phosphorylation of both MAPK and EGFR in a time-dependent manner. AG1478 pretreatment (1 h prior to CA) effectively inhibited the phosphorylation of both MAPK and EGFR (Fig. 2c). Although CA treatment activated AMPK in HepG2 cells, there were no significant differences in the cellular triglyceride content between the cells co-treated with compound C, a specific selective inhibitor of AMPK, and the cells treated only with CA (Fig. 2b, c).

CA regulates both the expression level and activity of PPARγ through EGFR/MAPK signaling in HepG2 cells

We also determined whether CA-stimulated EGFR/MAPK signaling plays a role in regulating PPARγ in HepG2 cells. We observed that the protein level of PPARγ in palmitate-induced cells was significantly reduced after the CA treatment, but was rescued by the pretreatment with either AG1478 or U0126 (Fig. 3a). Furthermore, the specific transcription factor DNA binding activity of PPARγ was significantly reduced after the CA treatment, but was rescued by pretreatment with either AG1478 or U0126. Consistently, the decreased nuclear protein levels of PPARγ in CA-treated cells were strongly elevated by pretreatment with the above inhibitors (Fig. 3b, c).

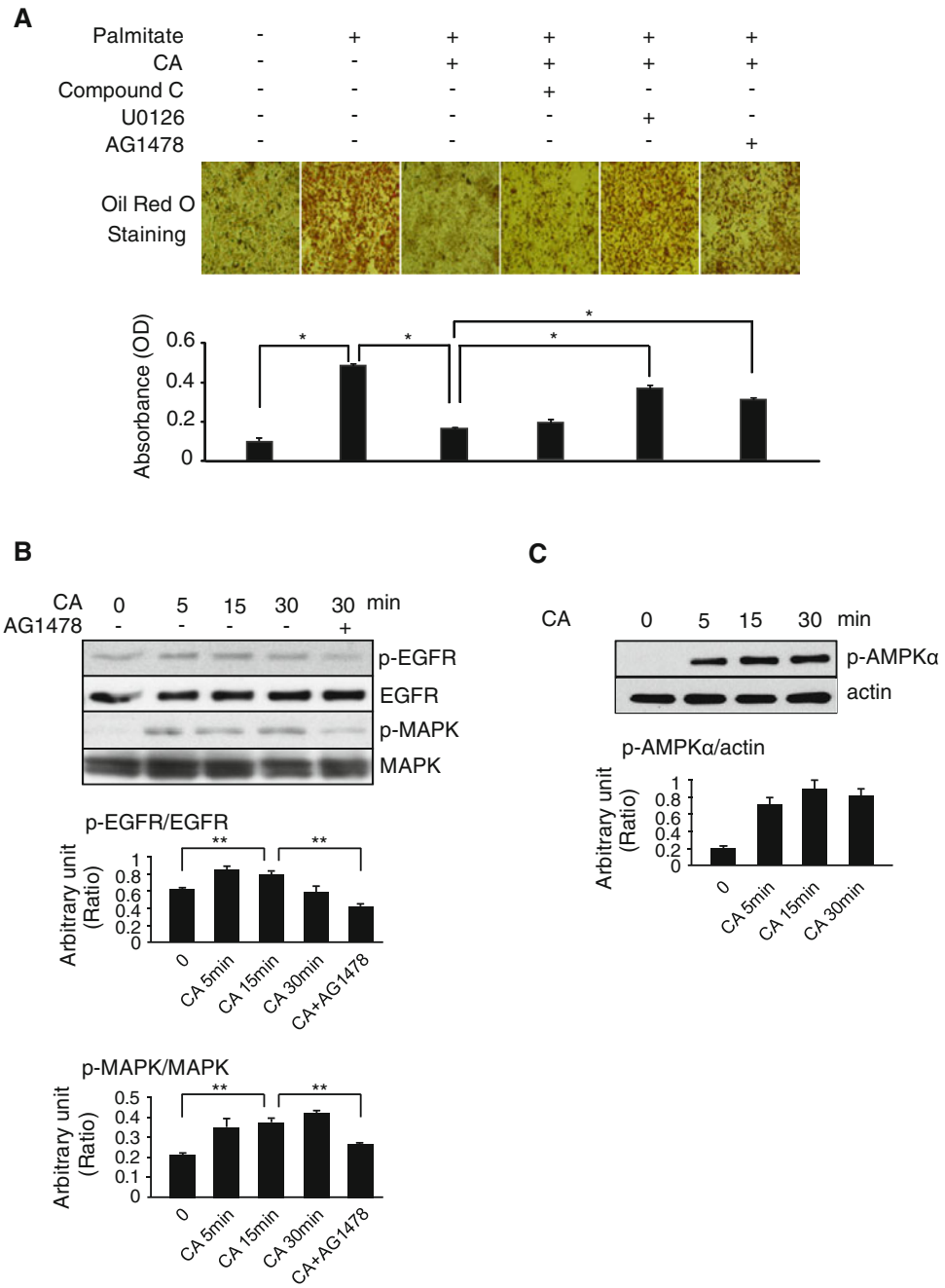

Fig. 2 Reduction of lipid accumulation in HepG2 cells by CA is associated with activation of MAPK and EGFR. **a** Both the EGFR and MAPK contribute to the inhibitory effects of CA on the cellular lipid accumulation induced by palmitate. HepG2 cells were induced by palmitate as described in the "Materials and methods". A concentration of 10 μM CA was added 1 day before the palmitate treatment. Then, 10 μM AG1478, 10 μM U0126, or 15 μM compound C was added, together with CA, as indicated. The cells were incubated for 18 h before the Oil Red O staining. **b** CA activated the EGFR/MAPK pathway in HepG2 cells. The 80% confluent HepG2 cells were starved in medium without FCS for 4 h. The cells were then treated with 20 μM CA for the indicated times. A concentration of 10 μM AG1478 was added 1 h prior to the CA treatment. **c** CA stimulated the phosphorylation of AMPKα in HepG2 cells. Cells were treated with CA for the indicated times as described in **b**. A 20-μg aliquot of total protein from each sample was used for the Western blot analysis. β-actin was evaluated as a protein loading control. All of the above experiments were repeated three times and representative results are shown. The quantitative data are presented as the means ± SD. $^{*}p < 0.05$, $^{**}p < 0.01$

Effects of CA on serum cytokine levels in *ob*/*ob* mice

Inflammatory cytokines are known to enhance the extent of liver injury [20, 21]. In the present study, a variety of cytokines such as IL-1β, IFN-γ, IL-12, IL-17, MCP-1, and MIP-1β were detected in the serum of control mice. In contrast, the serum of the mice fed the CA diet showed a significant decrease in the levels of these inflammatory cytokines. There were no significant differences in the levels of anti-inflammatory cytokines such as IL-10. The levels of TNF-α were also not significantly different between the CA and control groups (Table 1).

Discussion

The aim of the present study was to investigate the molecular and cellular mechanisms underlying the role of CA in lipid accumulation in hepatocytes. Oxidative stress contributes to the progression of steatosis to NASH by producing lipid peroxidation, inflammation, and fibrosis [22, 23]. Recently, Nrf2 was recognized as a target for the treatment of NAFLD [24, 25]. On the basis of the finding of our previous study, we thus hypothesized that CA exerts its effect on NAFLD by activating the Keap1/Nrf2 pathway. However, neither the protein levels of Nrf2 in the

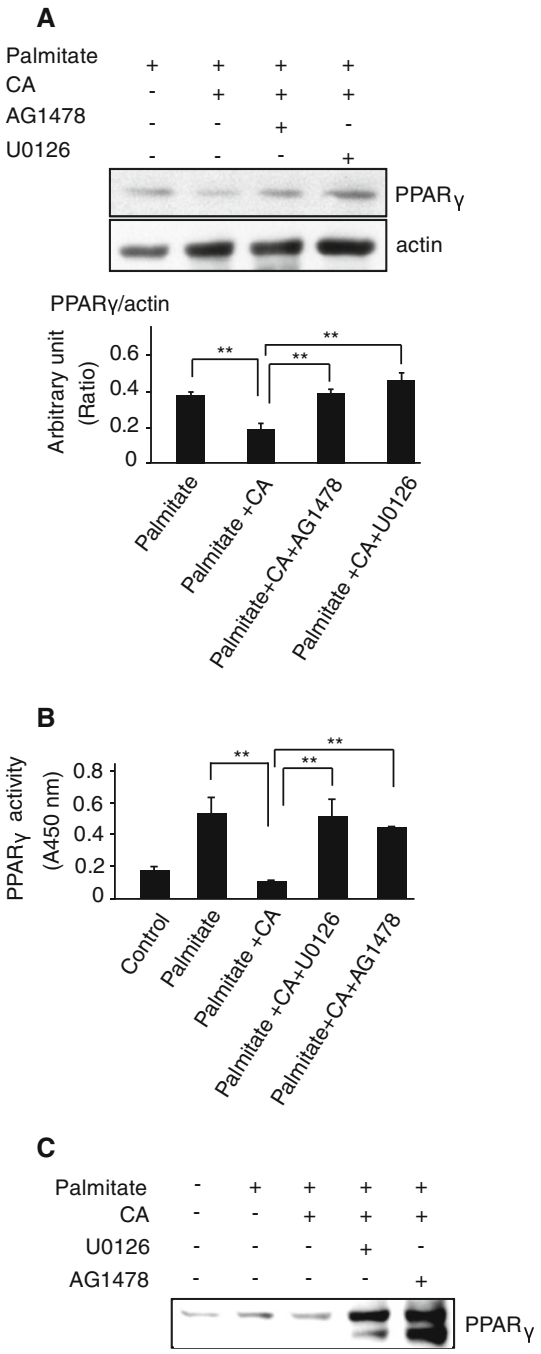

Fig. 3 CA decreased both the protein levels and activity of PPARγ through the EGFR/MAPK signaling pathway. Palmitate and CA were added to the cells as described in Fig. 2a. Then, 10 μM AG1478 or 10 μM U0126 was added as indicated. **a** The CA-stimulated EGFR/MAPK cascade decreased the total protein level of PPARγ. A 20-μg aliquot of total protein from each sample was used for the Western blot analysis. β-actin was evaluated as a protein loading control. **b**, **c** The CA-stimulated EGFR/MAPK cascade inhibited the activity of PPARγ. Analyses of both the protein levels and the activity of PPARγ were performed by using the nuclear fractions of the samples. PPARγ transcription factor assay was performed as described in the "Materials and methods". All of the above experiments were repeated three times and representative data are shown. The quantitative data are presented as the means ± SD. $^{**}p < 0.01$

nuclear fraction nor the production of GSH in the liver of CA-treated mice was elevated in comparison to control mice. Our present data therefore do not support the hypothesis that CA inhibits fat accumulation in the liver through the Nrf2/GSH pathway. However, because *ob*/*ob* mice present simple hepatic steatosis but not advanced stages of NAFLD such as NASH [26], further studies are needed to clarify the effect of CA on advanced NAFLD and to determine whether Keap1/Nrf2 signaling participates in the function of CA.

Our data indicate that CA-induced PPARγ reduction is involved in the prevention of lipid accumulation in hepatocytes. This is supported by a previous report indicating that liver-specific inhibition of PPARγ results in decreased hepatic steatosis [27]. We also demonstrated that the EGFR/MAPK signaling activated by CA is responsible for the suppression of both the protein expression and transcriptional activity of PPARγ. The EGFR is one of the potential upstream regulators of MAPK. It was reported that the ligand-dependent formation of EGFR homodimers or heterodimers with one of its homologs (ErbB2, ErbB3, and ErbB4) results in opposing effects on preadipocyte proliferation and differentiation [28]. In addition, activation of the EGFR/MAPK cascade plays an important role in the anti-obesity activity of evodiamine, a major component of traditional Chinese medicine [29, 30]. We herein demonstrated that the EGFR/MAPK pathway plays an important role in preventing lipid accumulation in the liver. Although the molecular mechanism by which CA activates the EGFR was not elucidated in the present study, an in vitro study showed that CA activated EGFR as early as 5 min post-stimulation, which suggests that CA possibly directly targets the EGFR through oligomerization or autophosphorylation, rather than an indirect mechanism. It is worth noting that EGFR activation is usually associated with an increased risk of cancer because it promote cell proliferation. However, so far, there have not been any reports of carcinogenic activity for CA. On the contrary, CA has been demonstrated to induce apoptosis in cancer cell lines [31, 32]. However, considering the possibility of the clinical application of CA, it is necessary to carefully determine whether there is any risk of cancer related to CA treatment.

In spite of the increased EGFR/MAPK signaling, our data from the present study showed that the phosphorylation of both AMPK and ACC was enhanced in the livers of mice fed a CA diet, and that this was accompanied by elevated levels of various hepatic metabolic molecules that participate in fatty acid β-oxidation. These data suggest that CA-stimulated AMPK plays a role in promoting fat consumption in the liver. However, the SREBP-1 levels in the nuclear fraction of the liver were not changed in the CA-treated mice. Although CA stimulated the phosphorylation of AMPK in HepG2 cells, a specific inhibitor of

AMPK did not block the inhibitory effects of CA on the cellular lipid accumulation induced by palmitate. These findings indicate that CA-induced AMPK activation does not directly suppress the short-term lipid accumulation induced by palmitate loading. On the other hand, the liver AMPK level regulates glucose homeostasis, in addition to regulating hepatic lipogenesis [6]. We previously reported that CA treatment improved the glucose intolerance in *ob*/*ob* mice [12]. Therefore, it is possible that CA indirectly blocks hepatocyte lipid accumulation in the long term by restoring insulin sensitivity, although future studies will be needed to determine whether this is the case.

Our previous data showed that CA treatment did not change the food intake of mice in comparison to controls [12]. These data suggest that CA protects against hepatic steatosis through a leptin-independent pathway, although further proof using other NAFLD animal models, such as MCD diet mice, is needed [33]. Leptin-deficient mice produce low levels of cytokines [34]. In the present study, the CA-treated mice showed even lower serum levels of many cytokines in comparison to the control mice. In particular, the serum levels of inflammatory cytokines like IFN-γ, MCP-1, MIP-1β, and GM-CSF were significantly lower in the CA-treated mice than in controls. So far, we do not know whether or not CA-induced PPARγ reduction relates to the changes of inflammation. It is also possible that the reduction of inflammatory cytokines in the in vivo experiments may occur due to the secondary effects of CA through body weight suppression, and this possibility should be examined in future studies. Our data above indicate that CA has potent anti-inflammatory activities even in *ob*/*ob* mice. Therefore, CA is expected to prevent the development of steatosis and to decrease the transition from NAFLD to steatohepatitis.

Acknowledgments This study was supported by a Grant-in-Aid for Strategic Medical Science Research Center (S1001001) from the Ministry of Education, Culture, Sports, Science and Technology of Japan. We thank Ms. A. Watanabe and Mr. K. Ishida for their valuable technical assistance.

Conflict of interest The authors declare that they have no conflict of interest.

References

1. Liu Q, Bengmark S, Qu S. The role of hepatic fat accumulation in pathogenesis of non-alcoholic fatty liver disease (NAFLD). Lipids Health Dis. 2010;9:42.
2. Musso G, Gambino R, Cassader M. Recent insights into hepatic lipid metabolism in non-alcoholic fatty liver disease (NAFLD). Prog Lipid Res. 2009;48(1):1–26.
3. Tessari P, Coracina A, Cosma A, Tiengo A. Hepatic lipid metabolism and non-alcoholic fatty liver disease. Nutr Metab Cardiovasc Dis. 2009;19(4):291–302.
4. Lelliott C, Vidal-Puig AJ. Lipotoxicity, an imbalance between lipogenesis de novo and fatty acid oxidation. Int J Obes Relat Metab Disord. 2004;28(Suppl 4):S22–8.
5. Viollet B, Guigas B, Leclerc J, Hebrard S, Lantier L, Mounier R, et al. AMP-activated protein kinase in the regulation of hepatic energy metabolism: from physiology to therapeutic perspectives. Acta Physiol (Oxf). 2009;196(1):81–98.
6. Zhang BB, Zhou G, Li C. AMPK: an emerging drug target for diabetes and the metabolic syndrome. Cell Metab. 2009;9(5):407–16.
7. Yang YM, Han CY, Kim YJ, Kim SG. AMPK-associated signaling to bridge the gap between fuel metabolism and hepatocyte viability. World J Gastroenterol. 2010;16(30):3731–42.
8. Gavrilova O, Haluzik M, Matsusue K, Cutson JJ, Johnson L, Dietz KR, et al. Liver peroxisome proliferator-activated receptor gamma contributes to hepatic steatosis, triglyceride clearance, and regulation of body fat mass. J Biol Chem. 2003;278(36):34268–76.
9. Kallwitz ER, McLachlan A, Cotler SJ. Role of peroxisome proliferators-activated receptors in the pathogenesis and treatment of nonalcoholic fatty liver disease. World J Gastroenterol. 2008;14(1):22–8.
10. Burns KA, Vanden Heuvel JP. Modulation of PPAR activity via phosphorylation. Biochim Biophys Acta. 2007;1771(8):952–60.
11. Bost F, Aouadi M, Caron L, Binetruy B. The role of MAPKs in adipocyte differentiation and obesity. Biochimie. 2005;87(1):51–6.
12. Wang T, Takikawa T, Satoh T, Yoshioka Y, Kosaka K, Tatemichi Y, et al. Carnosic acid prevents obesity and hepatic steatosis in *ob*/*ob* mice. Hepatol Res. 2011;40(6):605–12.
13. Aruoma OI, Halliwell B, Aeschbach R, Loligers J. Antioxidant and pro-oxidant properties of active rosemary constituents: carnosol and carnosic acid. Xenobiotica. 1992;22(2):257–68.
14. Satoh T, Kosaka K, Itoh K, Kobayashi A, Yamamoto M, Shimojo Y, et al. Carnosic acid, a catechol-type electrophilic compound, protects neurons both in vitro and in vivo through activation of the Keap1/Nrf2 pathway via S-alkylation of targeted cysteines on Keap1. J Neurochem. 2008;104(4):1116–31.
15. Tamaki Y, Tabuchi T, Takahashi T, Kosaka K, Satoh T. Activated glutathione metabolism participates in protective effects of carnosic acid against oxidative stress in neuronal HT22 cells. Planta Med. 2009;76(7):683–8.
16. Takahashi T, Tabuchi T, Tamaki Y, Kosaka K, Takikawa Y, Satoh T. Carnosic acid and carnosol inhibit adipocyte differentiation in mouse 3T3–L1 cells through induction of phase2 enzymes and activation of glutathione metabolism. Biochem Biophys Res Commun. 2009;382(3):549–54.
17. Vock C, Gleissner M, Klapper M, Doring F. Identification of palmitate-regulated genes in HepG2 cells by applying microarray analysis. Biochim Biophys Acta. 2007;1770(9):1283–8.
18. Gomez-Lechon MJ, Donato MT, Martinez-Romero A, Jimenez N, Castell JV, O'Connor JE. A human hepatocellular in vitro model to investigate steatosis. Chem Biol Interact. 2007;165(2):106–16.
19. Kasturi R, Joshi VC. Hormonal regulation of stearoyl coenzyme A desaturase activity and lipogenesis during adipose conversion of 3T3–L1 cells. J Biol Chem. 1982;257(20):12224–30.
20. Gao B. Cytokines, STATs and liver disease. Cell Mol Immunol. 2005;2(2):92–100.
21. Nanji AA, Jokelainen K, Rahemtulla A, Miao L, Fogt F, Matsumoto H, et al. Activation of nuclear factor kappa B and cytokine imbalance in experimental alcoholic liver disease in the rat. Hepatology. 1999;30(4):934–43.
22. Lewis JR, Mohanty SR. Nonalcoholic fatty liver disease: a review and update. Dig Dis Sci. 2010;55(3):560–78.

23. Musso G, Gambino R, Cassader M. Non-alcoholic fatty liver disease from pathogenesis to management: an update. Obes Rev. 2010;11(6):430–45.
24. Kathirvel E, Chen P, Morgan K, French SW, Morgan TR. Oxidative stress and regulation of anti-oxidant enzymes in cytochrome P4502E1 transgenic mouse model of non-alcoholic fatty liver. J Gastroenterol Hepatol. 2010;25(6):1136–43.
25. Chowdhry S, Nazmy MH, Meakin PJ, Dinkova-Kostova AT, Walsh SV, Tsujita T, et al. Loss of Nrf2 markedly exacerbates nonalcoholic steatohepatitis. Free Radic Biol Med. 2010;48(2):357–71.
26. Anstee QM, Goldin RD. Mouse models in non-alcoholic fatty liver disease and steatohepatitis research. Int J Exp Pathol. 2006;87(1):1–16.
27. Matsusue K, Haluzik M, Lambert G, Yim SH, Gavrilova O, Ward JM, et al. Liver-specific disruption of PPARgamma in leptin-deficient mice improves fatty liver but aggravates diabetic phenotypes. J Clin Invest. 2003;111(5):737–47.
28. Harrington M, Pond-Tor S, Boney CM. Role of epidermal growth factor and ErbB2 receptors in 3T3–L1 adipogenesis. Obesity. 2007;15(3):563–71.
29. Wang T, Wang Y, Yamashita H. Evodiamine inhibits adipogenesis via the EGFR–PKCalpha–ERK signaling pathway. FEBS Lett. 2009;583(22):3655–9.
30. Wang T, Wang Y, Kontani Y, Kobayashi Y, Sato Y, Mori N, et al. Evodiamine improves diet-induced obesity in a uncoupling protein-1-independent manner: involvement of antiadipogenic mechanism and extracellularly regulated kinase/mitogen-activated protein kinase signaling. Endocrinology. 2008;149(1):358–66.
31. Sharabani H, Izumchenko E, Wang Q, Kreinin R, Steiner M, Barvish Z, et al. Cooperative antitumor effects of vitamin D3 derivatives and rosemary preparations in a mouse model of myeloid leukemia. Int J Cancer. 2006;118(12):3012–21.
32. Tsai CW, Lin CY, Lin HH, Chen JH. Carnosic acid, a rosemary phenolic compound, induces apoptosis through reactive oxygen species-mediated p38 activation in human neuroblastoma IMR-32 cells. Neurochem Res. 2011;36(12):2442–51.
33. Leclercq IA, Farrell GC, Field J, Bell DR, Gonzalez FJ, Robertson GR. CYP2E1 and CYP4A as microsomal catalysts of lipid peroxides in murine nonalcoholic steatohepatitis. J Clin Invest. 2000;105(8):1067–75.
34. Siegmund B, Sennello JA, Lehr HA, Batra A, Fedke I, Zeitz M, et al. Development of intestinal inflammation in double IL-10 and leptin-deficient mice. J Leukoc Biol. 2004;76(4):782–6.